Supporting Information

Interfacial Charge Regulation in Solid-State UiO-67/$ZnIn_2S_4$/Pt Z-Scheme Heterojunctions for Efficient Photocatalytic Hydrogen Evolution

Bolong Qi[1], Rui Li[1], Haoran Jiang[2]*, Sheng Ye[2]*, Woon Yong Sohn[3] [4], Zhenhua Pan[1] [4]*

[1] Department of Applied Chemistry, Graduate School of Engineering, University of Hyogo, Himeji, Hyogo 671-2280, Japan.

[2] Anhui Engineering Research Center of Carbon Neutrality, The Key Laboratory of Functional Molecular Solids, Ministry of Education, College of Chemistry and Materials Science, Anhui Normal University, Wuhu, Anhui 241002, China.

[3] Department of Chemistry, Chungbuk National University, Chungdae-ro 1, Cheongju, Chungbuk 28644, Korea

[4] Chungbuk National University G-LAMP Project Group, Chungdae-ro 1, Cheongju, Chungbuk 28644, Korea

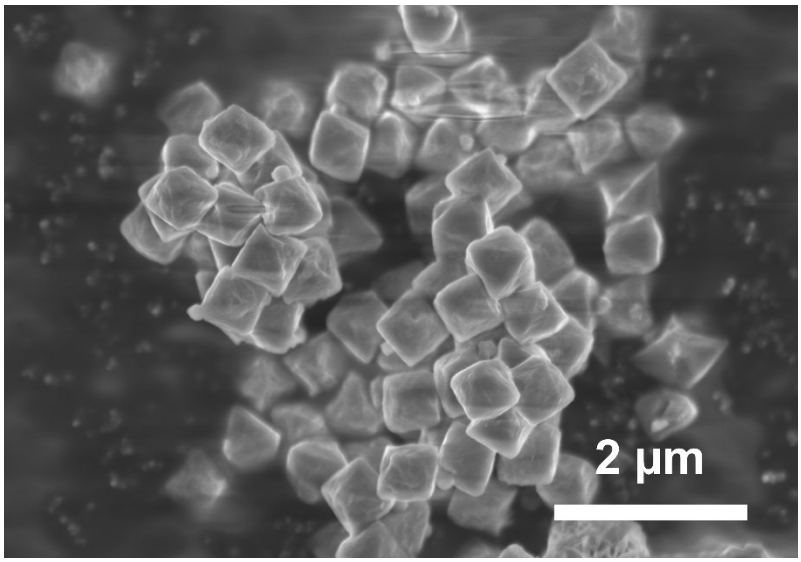

Figure S1. SEM image of the UIO-67.

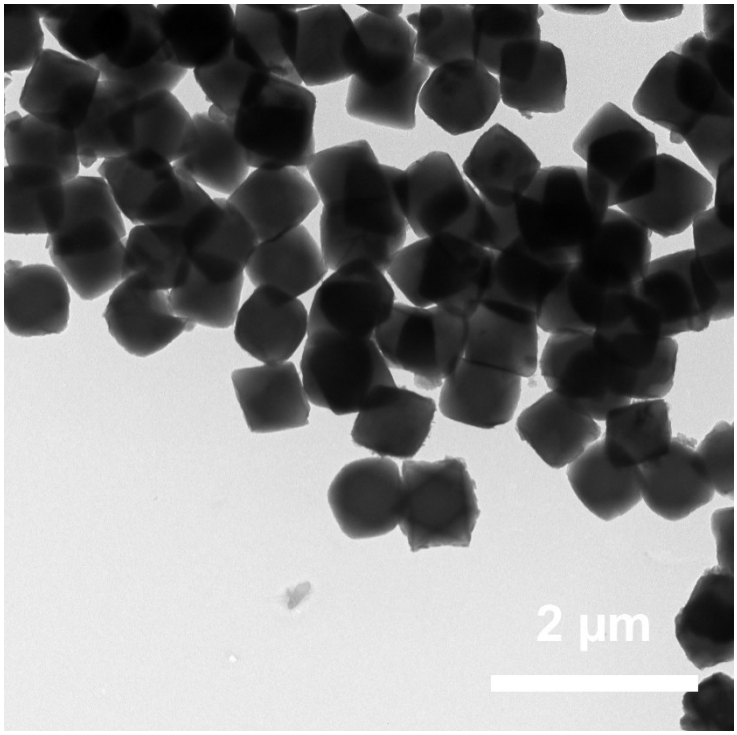

Figure S2. TEM image of the UIO-67.

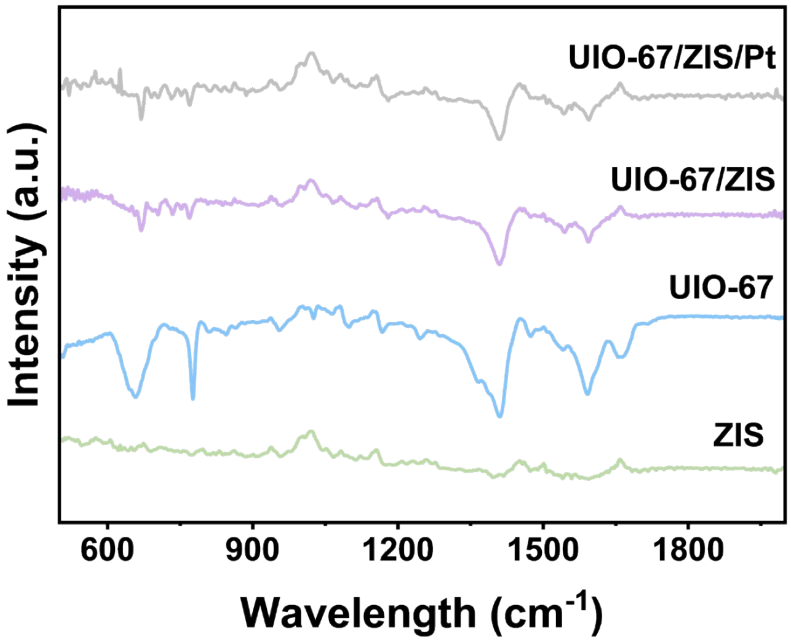

Figure S3. FTIR spectra of UIO-67, ZIS, UIO-67/ZIS, and UIO-67/ZIS/Pt.

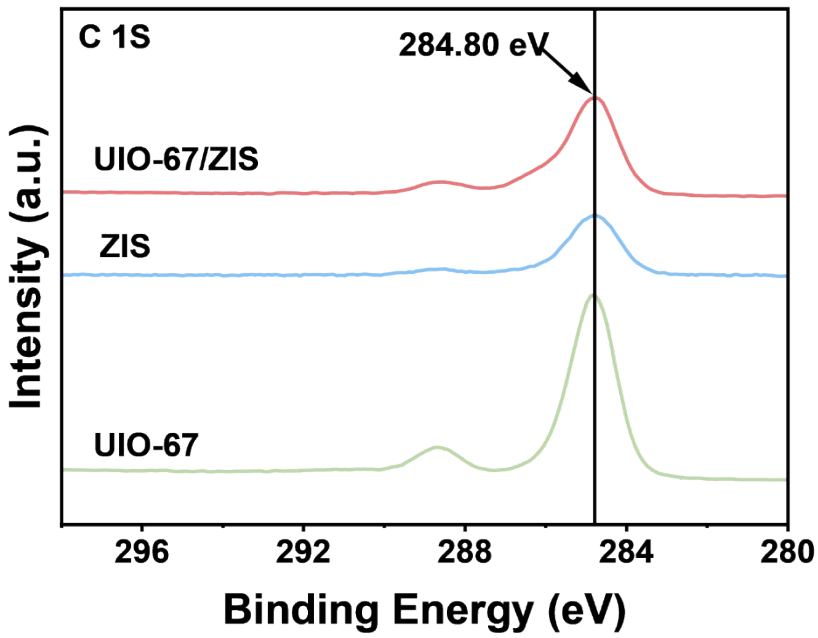

Figure S4. C 1S for UIO-67, ZIS and UIO-67/ZIS.

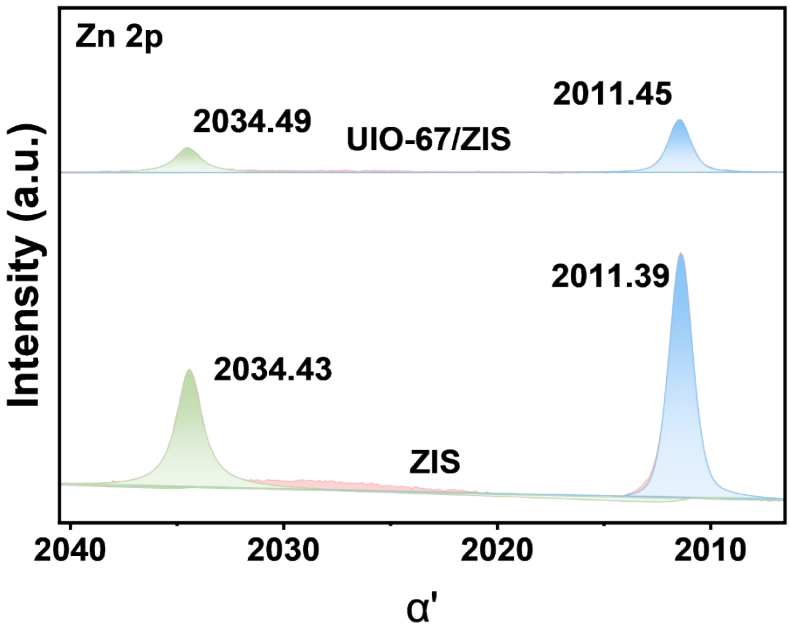

Figure S5. Modified Auger parameter (α') of Zn for ZIS and UIO-67/ZIS. α' = BE (photoelectron peak) + KE (Auger peak).

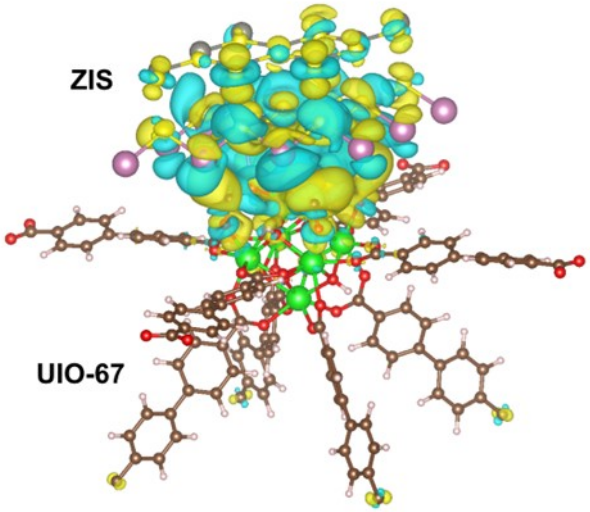

Figure S6. Charge density difference of the UiO-67/ZIS interface.

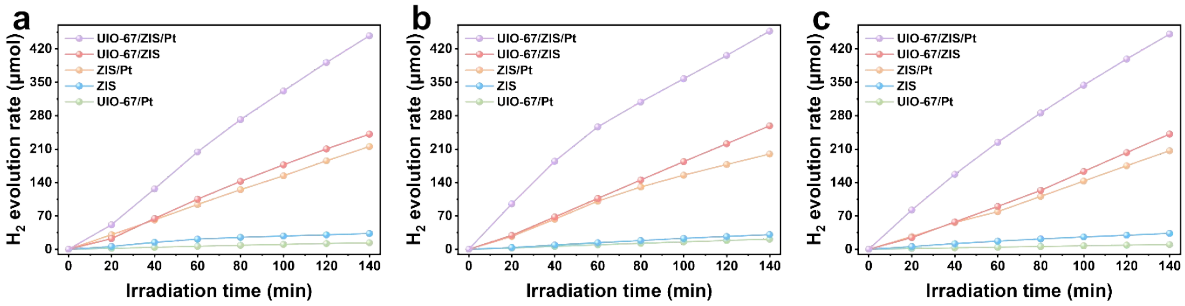

Figure S7. Hydrogen evolution data from three parallel experiments.

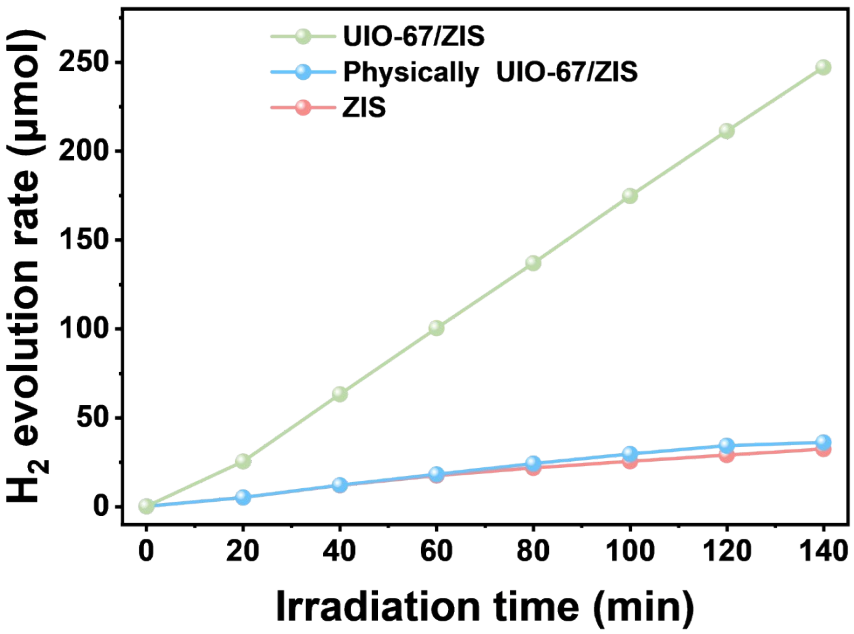

Figure S8. Photocatalytic hydrogen production experiment with physically mixed UIO-67/ZIS.

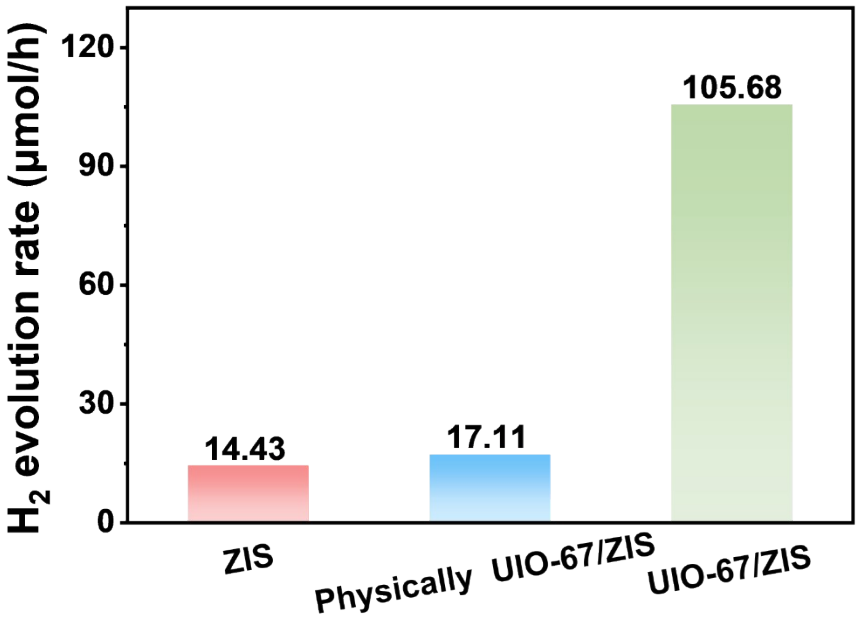

Figure S9. Comparison of the photocatalytic H_2 evolution rates of physically mixed UIO-67/ZIS.

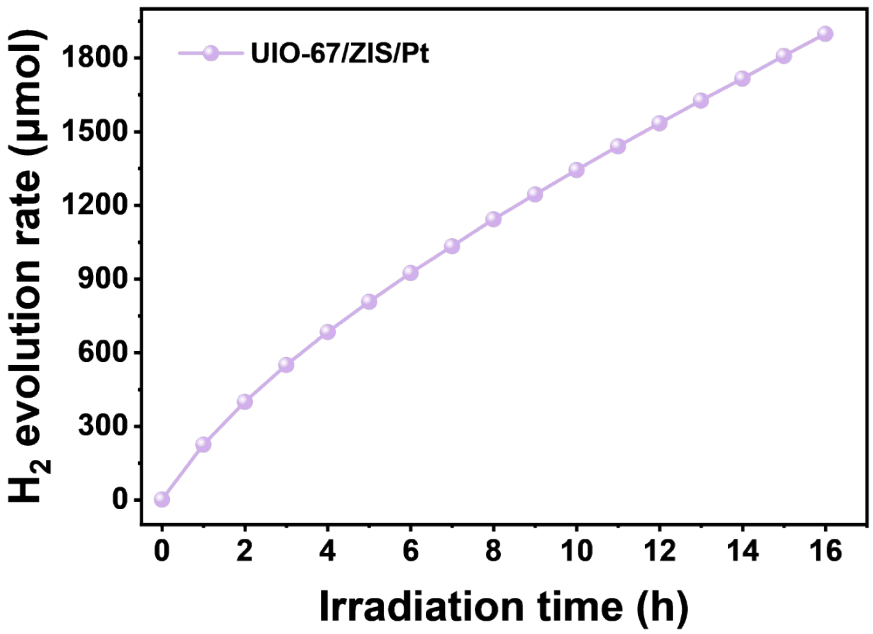

Figure S10. Continuous 16 h hydrogen production performance test.

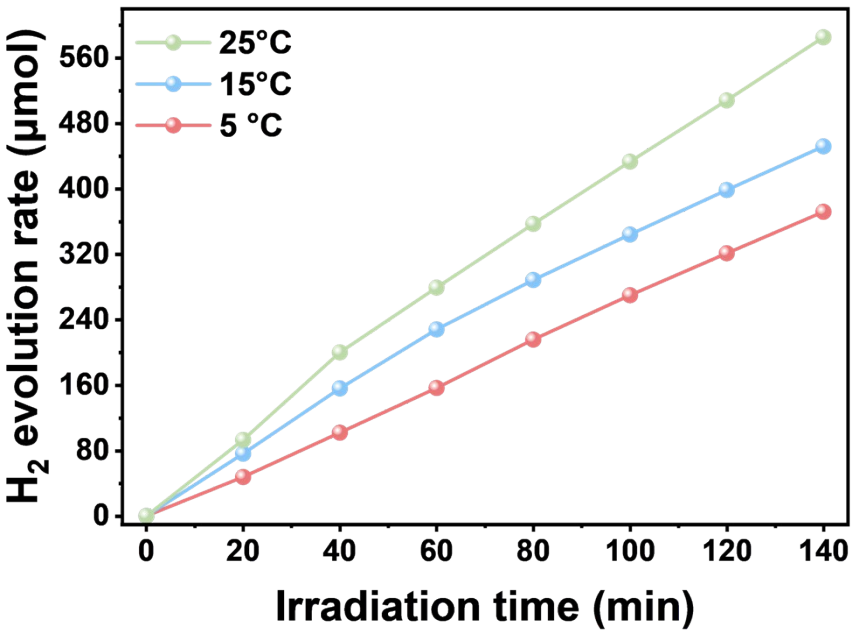

Figure S11. Photocatalytic hydrogen production tests at different temperatures. A higher temperature accelerated photocatalytic H_2 evolution because it enhances the kinetics of surface reactions and charge transfer processes.

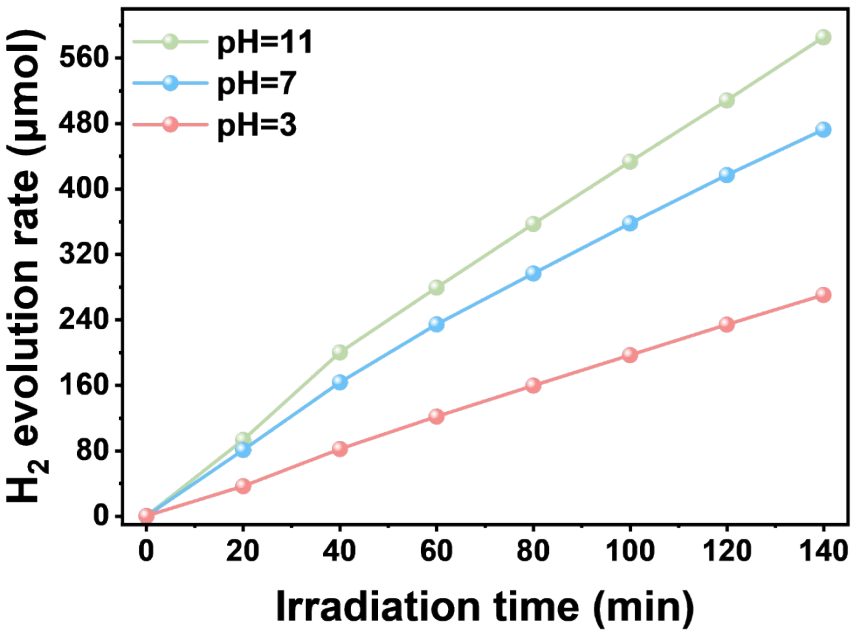

Figure S12. Photocatalytic hydrogen production tests at different pH. The enhanced H_2 evolution under alkaline conditions (pH ≈ 11) is mainly attributed to the deprotonated form of triethanolamine, which exhibits stronger hole-scavenging ability and improved adsorption on the catalyst surface, thereby suppressing charge recombination and promoting photocatalytic hydrogen production.[1]

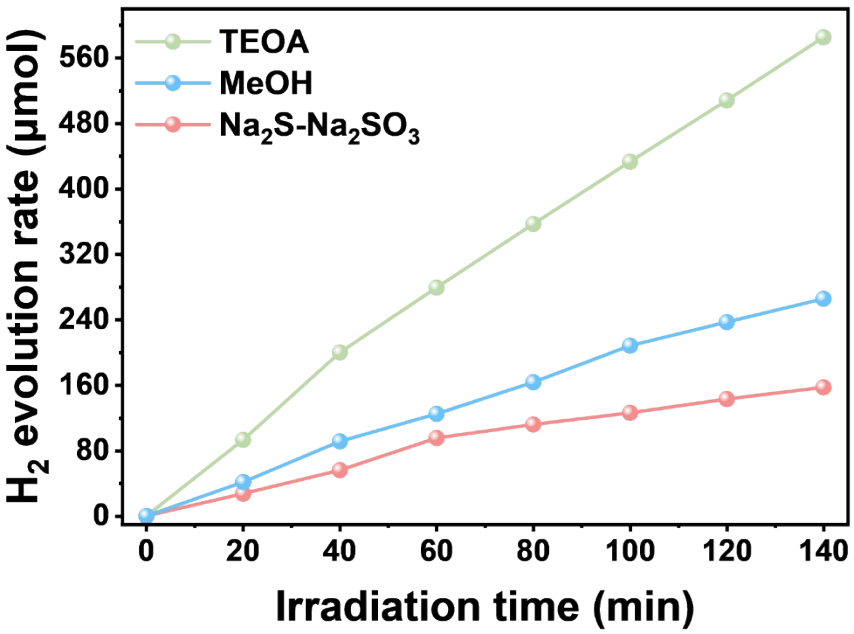

Figure S13. Photocatalytic hydrogen production tests at different solvents. The superior performance of TEOA is attributed to its strong hole-scavenging ability and good interaction with the catalyst, while methanol shows moderate activity and Na_2S–Na_2SO_3 suffers from side reactions that limit hydrogen evolution efficiency.

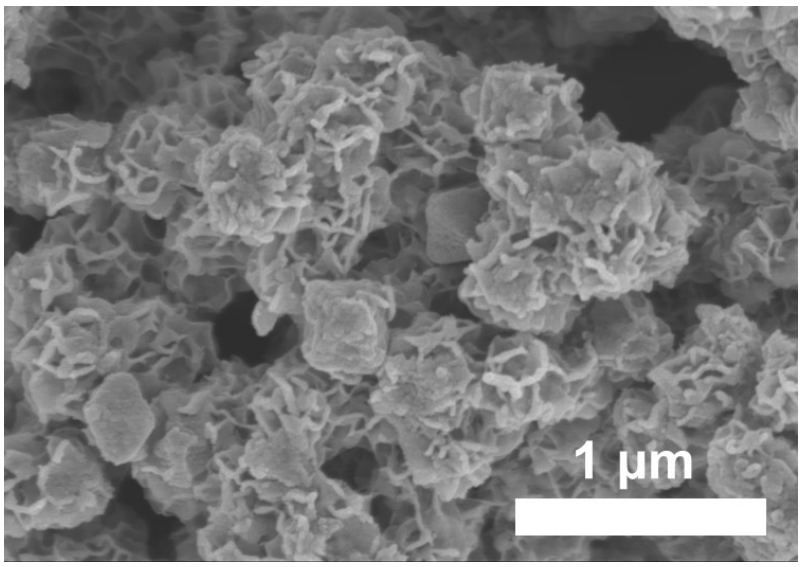

Figure S14. SEM image of UIO-67/ZIS/Pt after cyclic reaction.

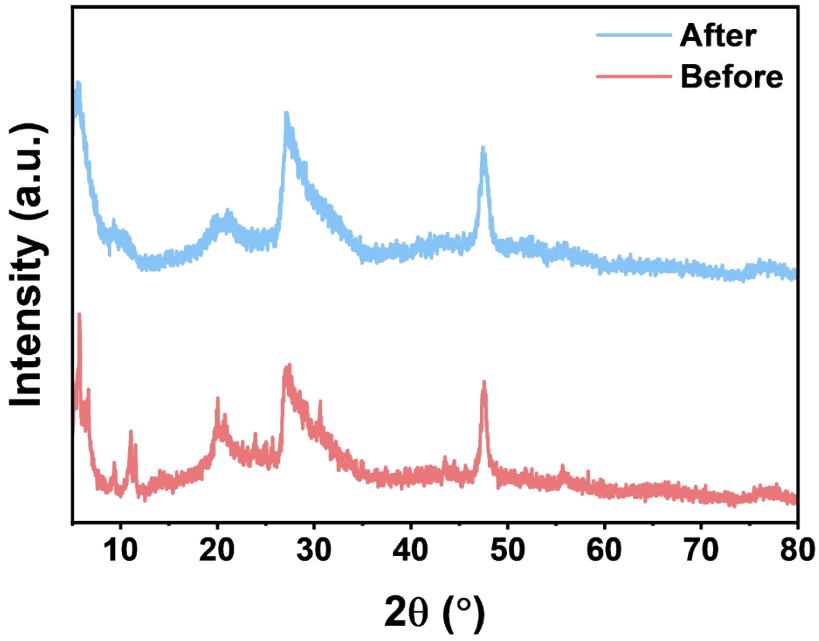

Figure S15. XRD of UIO-67/ZIS/Pt after cyclic reaction.

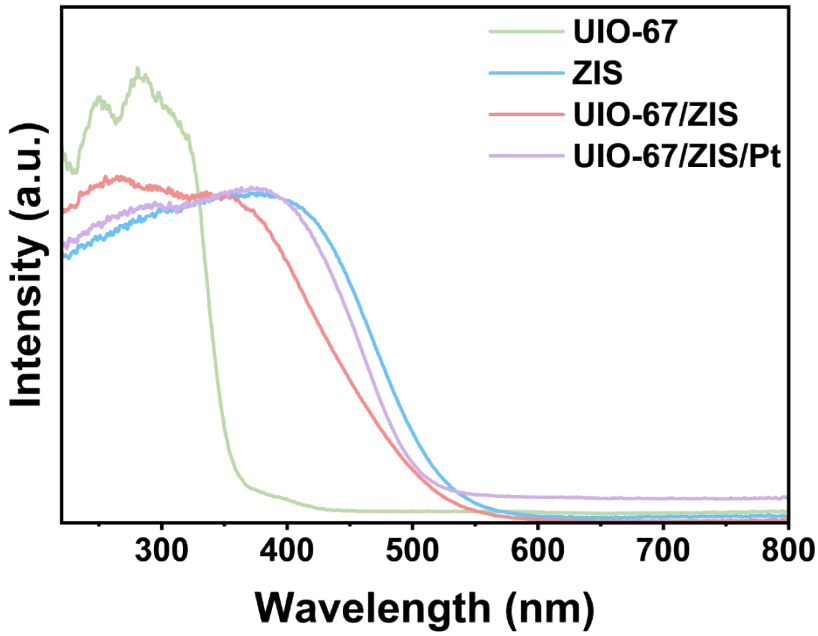

Figure S16. UV-vis diffuse reflectance spectra of UIO-67, ZIS, UIO-67/ZIS, and UIO-67/ZIS/Pt.

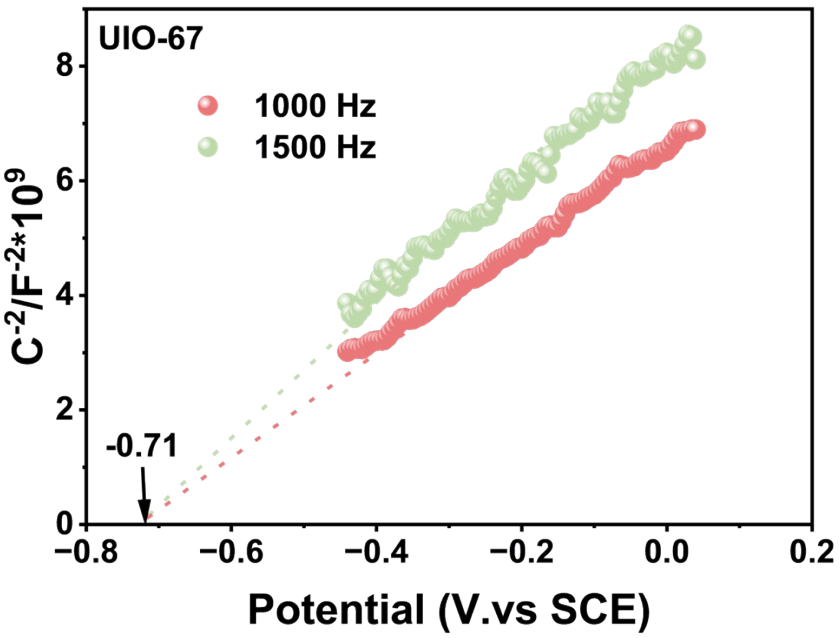

Figure S17. Mott-Schottky measurements of UIO-67.

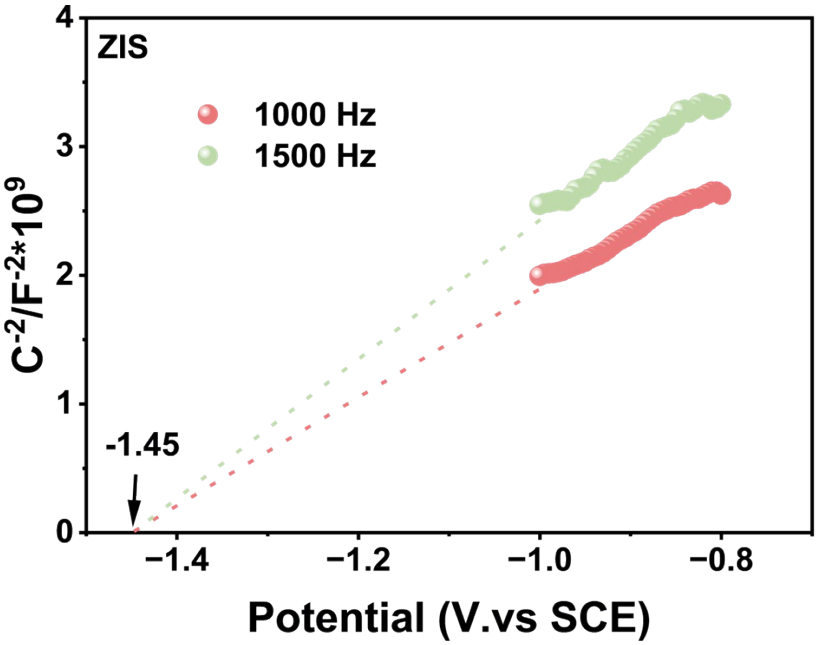

Figure S18. Mott-Schottky measurements of ZIS.

Table S1. COMSOL Multiphysics Simulation Parameters for UIO-67

Parameters	Values
Relative dielectric constant	4[2]
Band gap	3.6 eV
Electron affinity	4.3 V[3]
Effective state density, valence band	$1*10e^{24}$ m^{-3}[4]
Effective state density, conduction band	$1*10e^{23}$ m^{-3}[4]
Electron mobility	$1*10e^{-8}$ $[m^2/(V*s)]$[5]
Hole mobility	$1*10e^{-8}$ $[m^2/(V*s)]$[5]
Model width	150 nm
Model height	50 nm

Table S2. COMSOL Multiphysics Simulation Parameters for ZIS

Parameters	Values
Relative dielectric constant	4.7[6]
Band gap	2.5 eV
Electron affinity	3.8 V[6]
Effective state density, valence band	$2.3*10e^{25}$ m^{-3}[6]
Effective state density, conduction band	$1.8*10e^{24}$ m^{-3}[6]
Electron mobility	$1.07*10e^{-2}$ [m^2/(V*s)] [6]
Hole mobility	$1*10e^{-3}$ [m^2/(V*s)] [6]
Platinum is a work function	5.65 V
Model width	100 nm
Model height	10 nm

Table S3. Comparison of H_2 evolution performance over ZIS-based heterojunction photocatalysts.

Samples	Condition	H_2 evolution Rate (mmol.g-1.h-1)	AQY	stability	Ref.
UIO-67/ZIS/Pt	TEOA (Solar simulator)	7.97	5.94% at 380 nm	16 h	This work
$ZnIn_2S_4/FeWO_4$	Na_2SO_3 and Na_2S (Solar simulator)	3.53	19% at 420 nm	20 h	[7]
$Co_3O_4/ZnIn_2S_4$	TEOA ($\lambda > 420$ nm)	3.84	8.51% at 380 nm	20 h	[8]
K-g-$C_3N_4/ZnIn_2S_4$	TEOA (Solar simulator)	0.51		12 h	[9]
$ZnIn_2S_4$@Ni-MOF	TEOA ($\lambda > 420$ nm)	1.82		36 h	[10]
$Cu_2CoSnS_4/ZnIn_2S_4$	Methanol ($\lambda > 420$ nm)	4.90	17.76% at 350 nm	12 h	[11]
$CoFe_2O_4$@$ZnIn_2S_4$	TEOA ($\lambda > 420$ nm)	1.58	0.0047% at 420 nm	16 h	[12]
$ZnFe_2O_4$@$ZnIn_2S_4$/Au	TEOA ($\lambda > 420$ nm)	1.15	0.11 % at 420 nm	16 h	[13]
$ZnIn_2S_4$/TpPa-1	L-ascorbic acid ($\lambda > 420$ nm)	2.75	4.67 % at 420 nm.	24 h	[14]

$ZnIn_2S_4/Co_3Se_4$	Na_2SO_3 and Na_2S ($\lambda > 400$ nm)	2.46	2.11 % at 420 nm.	12 h	[15]
$ZnO/ZnIn_2S_4$	TEOA (Solar simulator)	1.99	7.4 % at 350 nm.	20 h	[16]
$ZnIn_2S_4$/h-BN	Na_2SO_3 and Na_2S (10 W LED lamp)	3.61	13.21 % at 365 nm	25 h	[17]

[1]. R. Yang, K. Song, J. He, Y. Fan, R. Zhu, *ACS Omega*, 2019, **4**, 11135–11140.

[2]. S. Balčiūnas, D. Pavlovaitė, M. Kinka, J.-Y. Yeh, P.-C. Han, F.-K. Shieh, K.C.-W. Wu, M. Šimėnas, R. Grigalaitis, J. Banys, *Molecules*, 2020, **25**, 1962.

[3]. X. Wang, W. Sun, Y. Tian, K. Dang, Q. Zhang, Z. Shen, S. Zhan, *Small*, 2021, **17**, 2100367.

[4]. M. Treger, C. König, P. Behrens, A.M. Schneider, *Phys. *Chem. Chem. Phys.*, 2023, **25**, 19013.

[5]. T.D. Musho, A.S. Yasin, *J. Electron. Mater.*, 2018, **47**, 3692.

[6]. N. Yang, Z. Yin, Z. Chen, C. Gao, Z. Cao, Y. Zheng, Z. Pan, H. Cao, S. Ye, Y. Xiong, *Angew. Chem. Int. Ed.*, 2025, **64**, e202502202.

[7]. D. Kong, X. Hu, J. Geng, Y. Zhao, D. Fan, Y. Lu, W. Geng, D. Zhang, J. Liu, H. Li, X. Pu, *Appl. Surf. Sci.*, 2022, **591**, 153256.

[8]. Y. Zhang, D. Chen, N. Li, Q. Xu, H. Li, J. Lu, *Appl. Surf. Sci.*, 2023, **610**, 155272.

[9]. Z. Cui, X. Kuang, R. Lv, X. Jin, F. Chen, Y. Kang, H. Zhang, H. Duan, B. Cao, Mater. Res. Bull., 2025, **192**, 113580.

[10]. K. Song, H. Lin, Q. Guo, F. Liao, C. Zeng, Appl. Catal. A, 2026, **710**, 120680.

[11]. Z. Shi, W. Jin, Y. Sun, X. Li, L. Mao, X. Cai, Z. Lou, Chin. J. Struct. Chem., 2023, **42**, 100201.

[12]. W. Ge, J. Song, S. Deng, K. Liu, P. Yang, Sep. Purif. Technol., 2024, **328**, 125059.

[13]. J. Song, W. Ge, S. Deng, J. Tang, S. Deng, P. Yang, Colloids Surf. A, 2025, **705**, 135705.

[14]. S.-D. Wang, L.-Y. Huang, L.-J. Xue, Q. Kang, L.-L. Wen, K.-L. Lv, Appl. Catal. B, 2024, **358**, 124366.

[15]. D. Zhang, D. Zhang, Y. Zhao, F. Zhao, X. Pu, H. Li, J. Liu, X.-Y. Ji, J. Alloys Compd.,

2024, **1008**, 176736.

[16]. L. Zhou, Q. Fang, M. Liu, S. Farhan, S. Yang, Y. Wu, Inorg. Chem., 2024, **63**, 21202.

[17]. P. Zou, Z. Wu, S. Ma, G. Cao, X. Jiang, H. Wang, Appl. Surf. Sci., 2025, **697**, 163017.